RNA (2001), *7*:1442–1453. Cambridge University Press. Printed in the USA.

DOI: 10.1017.S1355838201019070

The selenocysteine incorporation machinery: Interactions between the SECIS RNA and the SECIS-binding protein SBP2

JULIA E. FLETCHER,[1] PAUL R. COPELAND,[1] DONNA M. DRISCOLL,[1] and ALAIN KROL[2]

[1]Department of Cell Biology, Lerner Research Institute, Cleveland Clinic Foundation, Cleveland, Ohio 44195, USA
[2]Unité Propre de Recherche 9002 du Centre National de la Recherche Scientifique, Structure des Macromolécules Biologiques et Mécanismes de Reconnaissance, Institut de Biologie Moléculaire et Cellulaire, 67084 Strasbourg Cedex, France

ABSTRACT

The decoding of UGA as a selenocysteine (Sec) codon in mammalian selenoprotein mRNAs requires a selenocysteine insertion sequence (SECIS) element in the 3′ untranslated region. The SECIS is a hairpin structure that contains a non-Watson–Crick base-pair quartet with a conserved G.A/A.G tandem in the core of the upper helix. Another essential component of the Sec insertion machinery is SECIS-binding protein 2 (SBP2). In this study, we define the binding site of SBP2 on six different SECIS RNAs using enzymatic and hydroxyl radical footprinting, gel mobility shift analysis, and phosphate-ethylation binding interference. We show that SBP2 binds to a variety of mammalian SECIS elements with similar affinity and that the SBP2 binding site is conserved across species. Based on footprinting studies, SBP2 protects the proximal part of the hairpin and both strands of the lower half of the upper helix that contains the non-Watson–Crick base pair quartet. Gel mobility shift assays showed that the G.A/A.G tandem and internal loop are critical for the binding of SBP2. Modification of phosphates by ethylnitrosourea along both strands of the non-Watson–Crick base pair quartet, on the 5′ strand of the lower helix and part of the 5′ strand of the internal loop, prevented binding of SBP2. We propose a model in which SBP2 covers the central part of the SECIS RNA, binding to the non-Watson–Crick base pair quartet and to the 5′ strands of the lower helix and internal loop. Our results suggest that the affinity of SBP2 for different SECIS elements is not responsible for the hierarchy of selenoprotein expression that is observed in vivo.

Keywords: 3′ UTR; RNA–protein interactions; SECIS-binding protein 2; SECIS RNA; selenocysteine

INTRODUCTION

The 3′ untranslated regions (3′ UTRs) of eukaryotic mRNAs are generally not inert but rather constitute the repository of functional RNA elements, instrumental in controlling mRNA localization, stability, or translation. In this regard, the central role of RNA–protein interactions has been well documented. One such example in eukaryotes, where the binding of a protein to a 3′ UTR RNA hairpin is crucial to function, is the biosynthesis of selenoproteins. The selenoprotein translation machinery carries out two steps, selenocysteine biosynthesis and cotranslational incorporation of this amino acid (reviewed in Atkins & Gesteland, 2000). Selenocysteine is synthesized from serine on the $tRNA^{Sec}$, and the Sec-$tRNA^{Sec}$ is brought to the A-site of the ribosome by the specialized elongation factor mSelB/EFsec (Fagegaltier et al., 2000b; Tujebajeva et al., 2000).

Because selenocysteine is encoded by UGA, a mechanism functions to allow distinction of UGA/selenocysteine from UGA/stop codons. One molecular actor participating in this process is the selenocysteine insertion sequence (SECIS) element, an RNA hairpin residing in the 3′ UTR of selenoprotein mRNAs, that is mandatory for recognition of UGA as a selenocysteine codon (Berry et al., 1991). Structure probing (Walczak et al., 1996) and site-directed mutagenesis (Martin et al., 1998) provided secondary structure models for the SECIS RNAs, which consist of a hairpin composed of the two helices 1 and 2 separated by an internal loop. Worthy of note is that all SECIS RNAs can adopt the consensus secondary structure model despite a low

Reprint requests to: Alain Krol, Unité Propre de Recherche 9002 du Centre National de la Recherche Scientifique, Structure des Macromolécules Biologiques et Mécanismes de Reconnaissance, Institut de Biologie Moléculaire et Cellulaire, 15, Rue René Descartes, 67084 Strasbourg Cedex, France; e-mail: A.Krol@ibmc.u-strasbg.fr.

degree of sequence conservation. Structural features, such as the 13–15 bp conserved length of helix 2, were observed and tested experimentally (Walczak et al., 1996; Grundner-Culemann et al., 1999; R. Walczak & A. Krol, unpubl.). Additionally, structure–function studies established that four consecutive non-Watson–Crick base pairs (the base pair quartet) in the core of helix 2 constitute an important structural/functional motif that mediates selenoprotein mRNA translation (Walczak et al., 1996, 1998). This motif encompasses a central G.A/A.G base pair tandem that is conserved in all SECIS sequences examined so far. More recently, it was discovered that SECIS hairpins can indeed adopt two different apical structures, giving rise to SECIS form 2 possessing an additional helix 3 and a shorter apical loop than SECIS form 1 (illustrated in Fig. 3; Grundner-Culemann et al., 1999; Fagegaltier et al., 2000c). In addition, the presence of helix 3 in SECIS form 2 leads to formation of a second internal loop between helices 2 and 3. Interestingly, the invariant sequence AAR is always single stranded and well exposed in the apical region of the SECIS hairpin, whether in form 1 or 2.

Several attempts led to the isolation of various SECIS-binding proteins (Shen et al., 1995, 1998; Hubert et al., 1996; Fujiwara et al., 1999; Fagegaltier et al., 2000a), but the function of these proteins in selenocysteine incorporation was not verified. The purification, cloning, and functional analysis of the SECIS-binding protein 2 (SBP2) demonstrated that it binds specifically to the SECIS RNA and is a crucial component of the selenocysteine insertion machinery (Copeland & Driscoll, 1999; Copeland et al., 2000, 2001; Fletcher et al., 2000; Low et al., 2000). Mutations to the 5′ strand of the base pair quartet abolished SBP2 binding and selenocysteine incorporation (Copeland & Driscoll, 1999; Copeland et al., 2000), but the actual binding site of SBP2 on the SECIS RNA has not been identified. SBP2 binds not only the SECIS RNA, but also the specialized elongation factor mSelB/EFsec (Tujebajeva et al., 2000). The requirement for the two factors SBP2 and mSelB/EFsec introduces a major difference between eubacteria and eukaryotes. Indeed, whereas the eubacterial SelB carries out both the elongation translation factor and the RNA-binding activities, its eukaryotic counterpart is unable to bind the SECIS element directly and specifically (Fagegaltier et al., 2000b; Tujebajeva et al., 2000).

Domain dissection of SBP2 was recently reported, leading to the delineation of the RNA-binding domain and identification of important amino acids therein (Copeland et al., 2001). However, the RNA–protein interactions underlying the specific recognition of the SECIS RNA by SBP2 have not been investigated in great detail. In this study, we define the binding site of SBP2 on several SECIS RNAs using enzymatic and hydroxyl radical footprinting, gel mobility shift analysis, and phosphate-ethylation binding interference. A picture of the SECIS-SBP2 interactions emerges from our data, showing that the binding of SBP2 is limited to a region of the SECIS RNA centered around the internal loop and the non-Watson–Crick base pairs.

RESULTS

SBP2 interacts with various SECIS RNAs

The recombinant rat SBP2 was shown to bind specifically to the rat phospholipid hydroperoxide glutathione peroxidase (PHGPx) SECIS element in a mobility shift assay (Copeland et al., 2001). We tested the ability of SBP2 to interact with five other ^{32}P-labeled SECIS RNAs representing both form 1 and form 2 structures from a variety of species as illustrated in Figure 3. Retarded bands were obtained with each of the tested SECIS RNAs, indicating that SBP2 can form RNA–protein complexes stable enough to sustain electrophoresis conditions. Representative gels are shown for the binding of SBP2 to the mouse Sel15 (Fig. 1A) and human SelN (Fig. 1B) SECIS RNAs. Figure 1A,B also shows that a second complex of slower mobility (complex B, lanes 7 and 8) appeared with higher amounts of SBP2, which is likely due to self-association of SBP2, as was observed previously in glycerol gradient sedimentation of recombinant SBP2 (Copeland et al., 2001).

To determine the affinity of SBP2 for the different SECIS RNAs, the apparent K_ds for binding were derived from mobility shift experiments, as detailed in Materials and Methods. As shown in Figure 1C, SBP2 has a similar affinity for the PHGPx, type 1 deiodinase (5′ DI), and Sel15 SECIS elements, with apparent K_d values of 94.5 nM, 87.5 nM, and 97.0 nM, respectively. However, for the GPx, SelP, and SelN SECIS elements, higher apparent K_ds ranging from 196 to 133 nM were observed. The full range of K_d values spans 2.24-fold, indicating that SBP2 binds the SECIS RNAs with affinities ranging within the same order of magnitude. From these experiments, we conclude that rat SBP2 interacts specifically with a variety of SECIS elements and that the SBP2 binding site is conserved across several mammalian species.

SECIS RNA regions protected by SBP2

Earlier experiments using crosslinking assays delineated some of the structural features required for SBP2 to bind the PHGPx SECIS RNA (Lesoon et al., 1997; Copeland & Driscoll, 1999). Crosslinking of SBP2 was greatly reduced or abolished by the shortening of helix 1 or by a base substitution in the non-Watson–Crick base pair quartet. To obtain more substantial information and to analyze in particular how SBP2 lies on the SECIS RNA, we carried out RNA footprinting assays. Protection of the RNA against mild RNase T1 or T2 hydrolysis was initially investigated to broadly localize the binding site. RNase T1 cleaves after Gs, mostly in

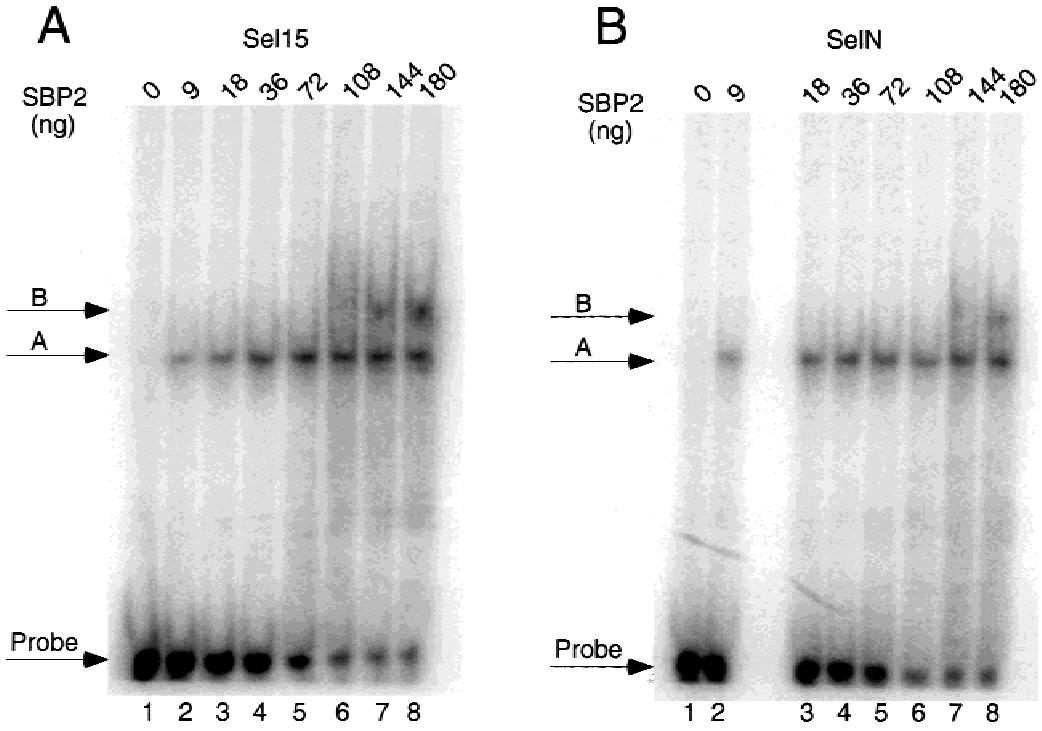

C

SBP2 interactions with the SECIS RNAs

SECIS	Apparent Kd (nM ± S.E.)
5'DI	87.5 ± 7.5
PHGPx	94.5 ± 0.5
Sel15	97.3 ± 11.2
SelN	133.0 ± 26.5
SelP	150.4 ± 6.1
GPx	196.5 ± 14.6

FIGURE 1. SBP2 binds a variety of SECIS RNAs. The mobility shift assays are shown for complexes formed between SBP2 and [α-^{32}P]-labeled Sel15 (**A**) and SelN (**B**) SECIS RNAs. The amount of SBP2 used in the assays is indicated above the lanes. Two complexes (A and B) form. Complex B, which appears with higher amounts of protein, may be due to SBP2 self-association. **C:** The apparent K_d values in nM were determined as described in Materials and Methods. S.E. is the standard error.

single strands under the conditions employed, and RNase T2 hydrolyzes single strands without marked base specificity. Representative gels are shown in Figure 2 for the SelN and SelP RNAs. In the SelN-SBP2 complex, the G10-A11 and G46-A47 phosphodiester bonds were protected against RNase T1 digestion (Fig. 2A, compare lanes 4 and 5 with lanes 9 and 10). RNase T1 was prevented from cleaving the G11-A12 and G54-A55 bonds in the SelP-SBP2 complex, but cleavage of the G58-C59 bond was enhanced in the complex (Fig. 2B, compare lanes 4 and 5 with lanes 9 and 10), suggesting that this region is not in contact with SBP2. Gels are not displayed for the other RNAs, but protections for the Sel15, 5′ DI, and PHGPx SECIS RNAs are schematized in Figure 3.

To obtain more detailed information about the areas protected by SBP2, we turned to hydroxyl radical-mediated cleavages of the RNA phosphodiester bonds. Fe/EDTA generates hydroxyl radicals that induce cleavages of the ribose rings. Because these radicals are smaller than RNases, and do not diffuse off the production site, they provide a good picture of the RNA regions in an RNA–protein complex that are protected against their attack. Representative gels of the protections afforded by SBP2 to the 5′ DI and Sel15 SECIS RNAs are displayed in Figure 4A,B, and the data for the remaining SECIS elements are summarized in Figure 3. Predominantly uniform cleavage occurred in the absence of SBP2, indicating that the riboses are accessible to the solvent (lanes 3 in Fig. 4). In the presence of SBP2, several riboses became protected. For 5′ DI, these map between positions U13-G20, A24-U28, and C59-U64 (Fig. 4A, lane 4). For Sel15 (Fig. 4B), protection was observed at U1-G4

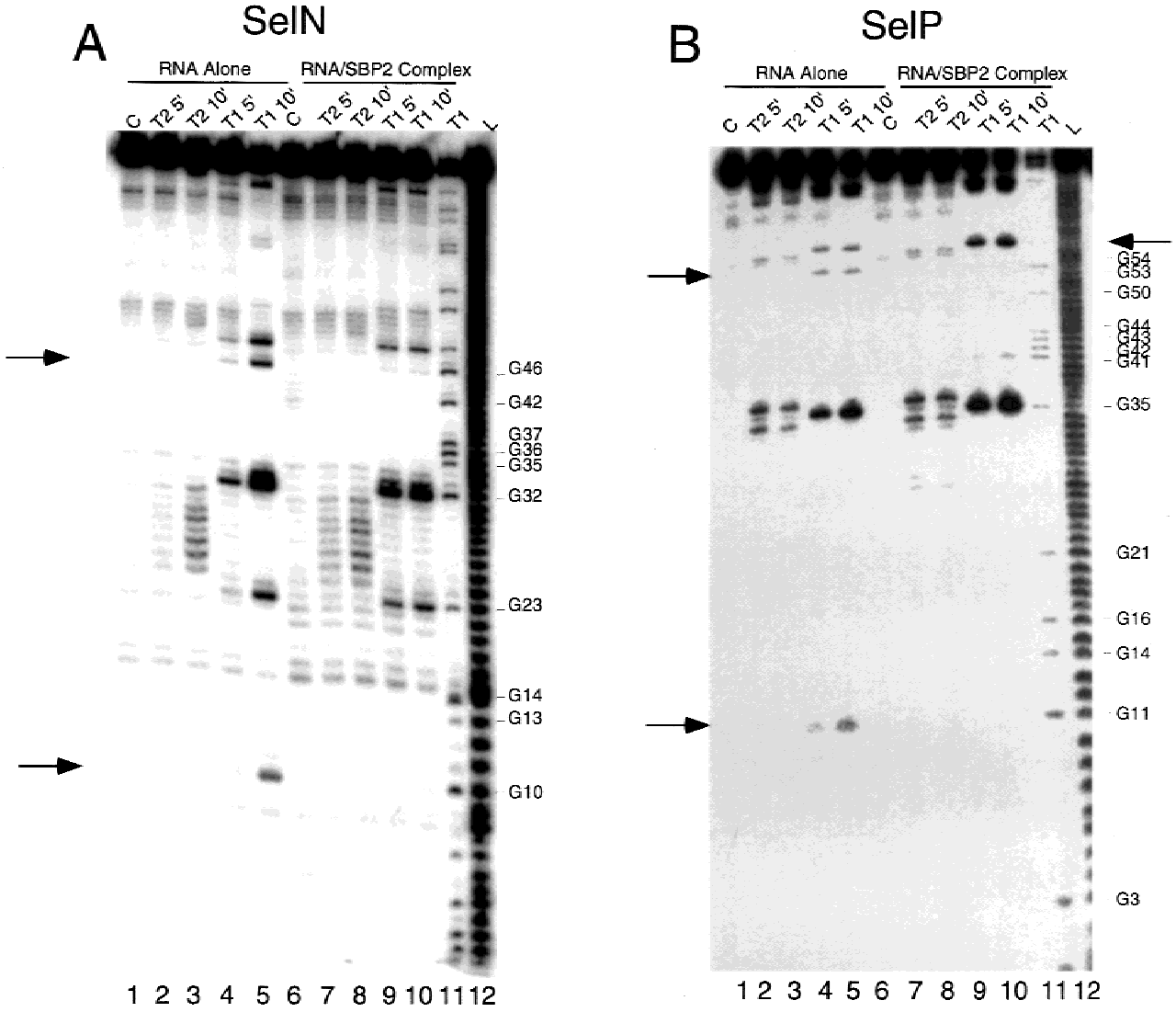

FIGURE 2. Enzymatic footprinting of SECIS RNA-SBP2 complexes. **A:** The 5′-end-labeled SelN SECIS RNA, alone or complexed with SBP2, was submitted to mild RNase T1 or T2 digestion for the periods of time indicated above the lanes. C: control without enzyme; T1 (lane 11): RNase T1 ladder; L (lane 12): alkaline ladder. The guanine positions indicated on the right correspond to the numbering in Figure 3. **B:** Identical experiments were performed with the SelP SECIS RNA. Arrows point to the positions discussed in the text.

and U54-G55, with weaker protection at G12-G14 (lane 4). Based on these results, the SECIS domains in 5′ DI and Sel15 that are protected by SBP2 reside in the proximal part of the hairpin, comprising portions of the 5′ strands of helix 1, and both strands of the bottom half of helix 2. Nearly identical regions of protection were observed with the other SECIS elements as illustrated in Figure 3.

The internal loop and the non-Watson–Crick base pairs are important features for the binding of SBP2

The protected ribose phosphate bonds include regions that are highly conserved between different SECIS RNAs: the G.A/A.G tandem in the non-Watson–Crick base pair quartet, and the internal loop 1 with the single-stranded A (numbered A9 in the GPx SECIS; see Fig. 3). This finding prompted us to determine whether these features constitute nucleotide sequence and/or structural determinants for SBP2 binding. We chose to analyze mutants in the GPx SECIS that have previously been analyzed for their ability to function in Sec insertion (Walczak et al., 1998). A series of mutations in the non-Watson–Crick base pair quartet was tested that either converted it into four Watson–Crick base pairs (n-W-C/W-C), or introduced point mutations into the G.A/A.G base pair tandem to generate the **A.G**/**G.A**, **A**.A/A.G, or G.A/A.**A** base pairs (mutated bases in bold). Only mutant G.A/A.**A** was capable of binding, as it led

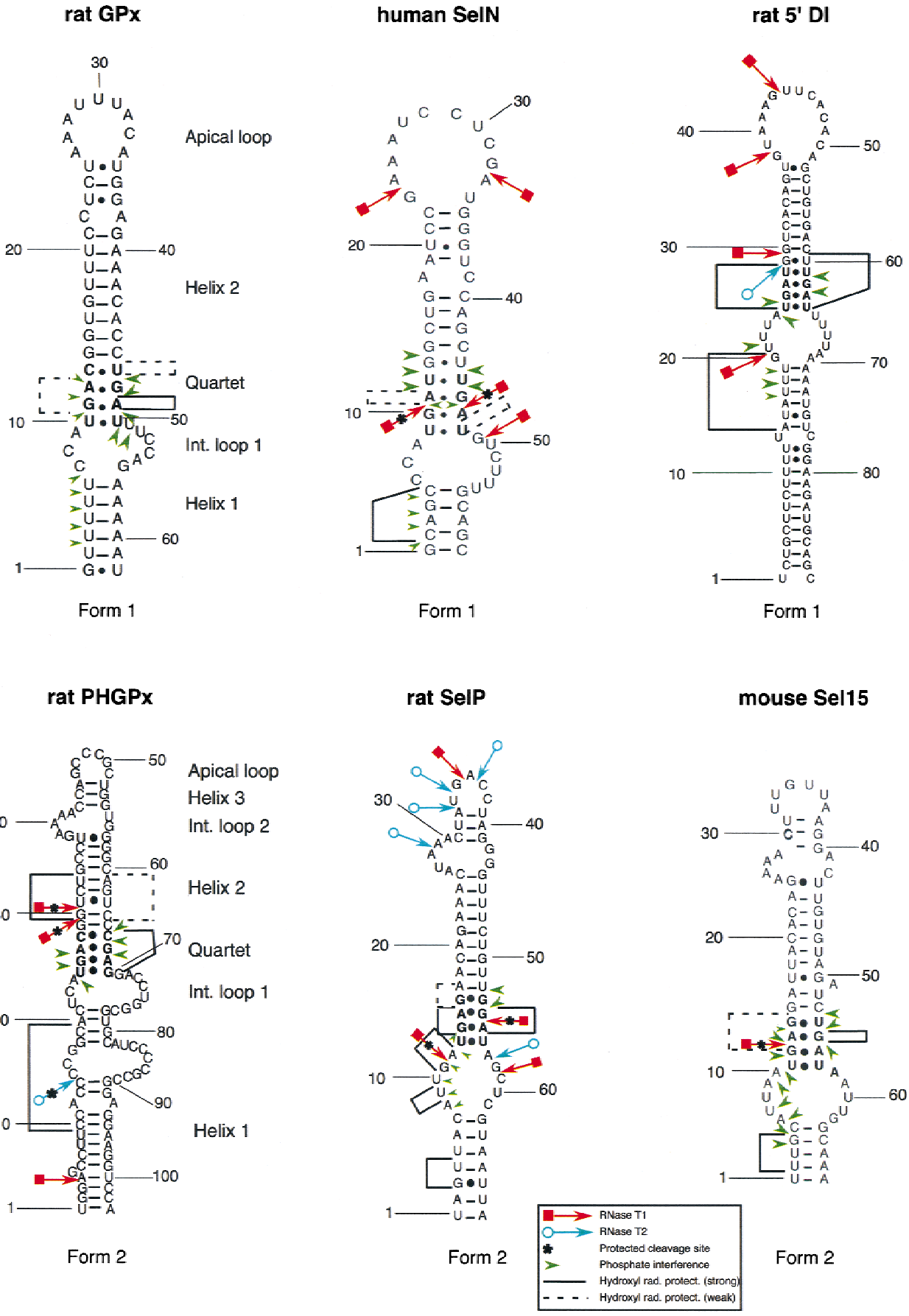
rat GPx
Apical loop
Helix 2
Quartet
Int. loop 1
Helix 1
Form 1
human SelN
Form 1
rat 5' DI
Form 1
rat PHGPx
Apical loop
Helix 3
Int. loop 2
Helix 2
Quartet
Int. loop 1
Helix 1
Form 2
rat SelP
Form 2
mouse Sel15
Form 2
RNase T1
RNase T2
Protected cleavage site
Phosphate interference
Hydroxyl rad. protect. (strong)
Hydroxyl rad. protect. (weak)

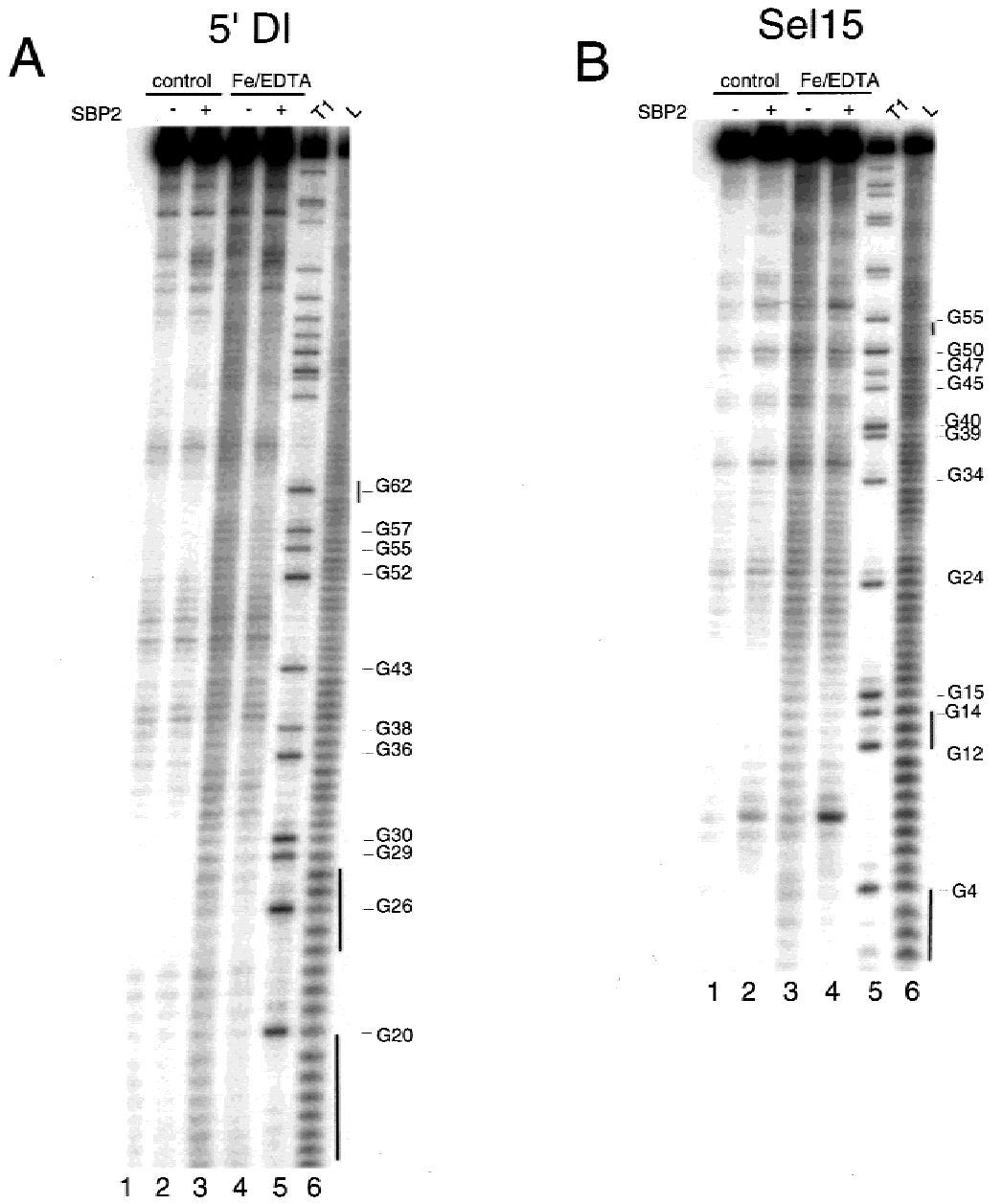

FIGURE 4. Protection afforded by SBP2 to SECIS RNAs against ribose modification. **A:** Hydroxyl radical footprint analysis of 5′-end-labeled Sel15 SECIS RNA. The RNA was incubated in the absence (lanes 1 and 2) or presence (lanes 3 and 4) of Fe(II)-EDTA induced hydroxyl radicals. SBP2 was added in lanes 2 and 4. T1 (lane 5): RNase T1 ladder; L (lane 6): alkaline ladder. The guanine positions refer to the numbering in Figure 3; bars on the right display the protected regions also shown in Figure 3. **B:** The 5′ DI SECIS RNA-SBP2 complex was treated as in **A**.

FIGURE 3. Summary of the results of the protection and interference experiments on the secondary structure of the different SECIS RNAs. RNase cleavages are indicated by arrows; RNase T1: solid red squares; RNase T2: open blue circles. Cleavage sites protected by SBP2 are marked with an asterisk. The regions containing the riboses protected against hydroxyl radical attack are indicated by solid or broken (weaker protection) black lines. Green arrowheads depict the phosphates that interfere with the binding to SBP2. The size of the arrowheads represents the intensity of the protection observed. Shown are the GPx, SelN, and 5′DI (form 1) and PHGPx, Sel15, and SelP (form 2) SECIS RNAs that were analyzed in this work. The non-Watson–Crick base pairs are in bold.

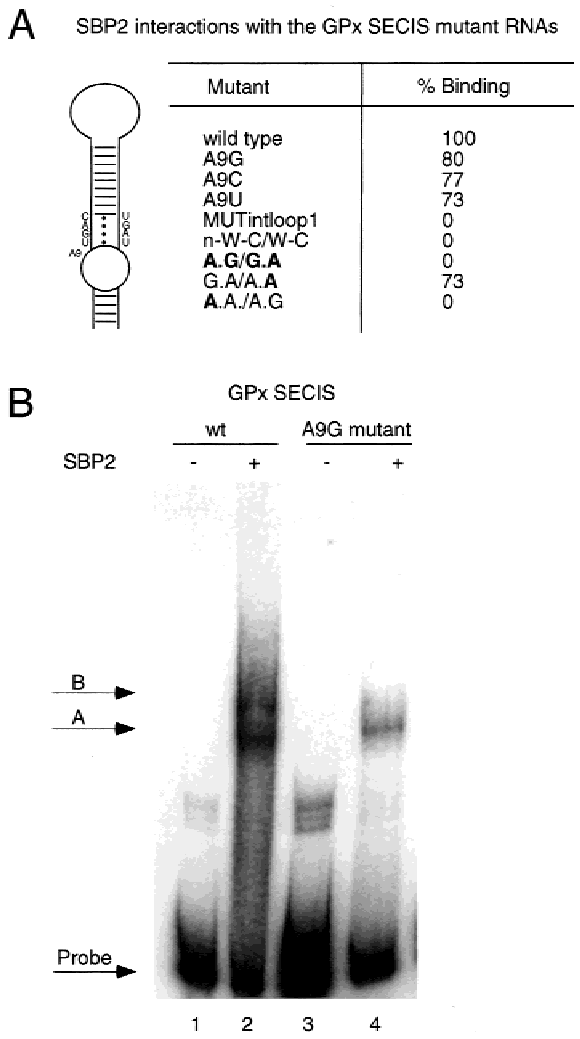

FIGURE 5. Electrophoretic mobility shift assay of SBP2 with GPx SECIS mutants. **A:** Recombinant C-terminal SBP2 was added to 150,000 cpm of each [α-^{32}P] labeled GPx SECIS RNA (wild-type and the mutants listed), and the complexes were resolved by 4% nondenaturing gel electrophoresis. The slower mobility complex B was quantified by PhosphorImager analysis and the binding efficiency is expressed as the percent of total probe RNA that was shifted, normalized to the wild-type probe. A schematic of the GPx SECIS core is shown on the left. **B:** Representative electrophoretic mobility shift assay of wild-type and mutant A9G GPx SECIS RNA. Note that SBP2 forms two distinct complexes (denoted A and B), the larger of which (B) is likely due to SBP2 self-association.

to a retarded complex retaining 73% of the wild-type signal (Fig. 5A). In contrast, the other three mutations were severely deleterious, as they abolished formation of the retarded complex (Fig. 5A). We investigated the importance of the identity of the single-stranded base at the GPx position 9 that is occupied by an A in the majority of the SECIS elements (Grundner-Culemann et al., 1999; Fagegaltier et al., 2000c). Figure 5B shows an example of the effects of GPx SECIS mutant A9G on SBP2 binding as evaluated by the mobility shift assay (compare lanes 2 and 4). In fact, the A9G A9C or A9U changes only moderately reduced the signal of the retarded complex to 80%, 77%, and 73% of the wild-type intensity, respectively (Fig. 5A). Last, we asked what would be the consequence of closing internal loop 1 on SBP2 binding. This closure was achieved by introducing Watson–Crick base pairs (MUTintloop1 in Fig. 5A). Remarkably, the lack of an internal loop had a dramatic effect, as the mutation abolished the retarded complex.

From these experiments, we conclude that two features in the GPx SECIS RNA constitute nucleotide sequence and/or structural determinants important for binding of SBP2: the internal loop 1 and all or part of the non-Watson–Crick base pair quartet. This finding was supported by the U25C and G67A transitions engineered in the PHGPx SECIS base pair quartet (see Fig. 3 for the localization) that eliminated SBP2 binding and Sec insertion (Lesoon et al., 1997; V. Stepanik, P.R. Copeland, & D.M. Driscoll, unpubl. data). Remarkably, the single U-to-C change was inhibitory to complex formation, whereas the G-to-A substitution was innocuous, in line with the G.A/A.**A** mutation carried out in the GPx SECIS.

Phosphate ethylation-binding interference

To obtain further information on likely points of contact between SBP2 and the SECIS RNA backbone, ethylnitrosourea (ENU) was used to probe the SBP2-SECIS interaction using the modification interference assay. ENU ethylates the phosphate oxygens, and interference of SBP2 binding by a modification at a given phosphate may result from an essential protein–RNA contact. 5′-end labeled ENU-modified PHGPx, 5′ DI, SelN, Sel15, SelP, and GPx SECIS RNAs were prepared at a ratio of approximately one ethyl group per molecule, and then complexed to SBP2. Bound and free RNA populations were separated on nondenaturing gels, cleaved at ethylated phosphate positions by high pH treatment, and fractionated on sequencing gels. The positions where modification interfered with SBP2 binding were identified by comparison of the free and bound lanes, and the results are summarized in Figure 3. In the free RNAs, all the phosphodiester bonds were susceptible to ethylation (as shown for PHGPx and GPx in Fig. 6, lanes 5). Inspection of the bound fractions (Fig. 6, lanes 6) led to the following observations. Strong interference occurred at the 3′ phosphates of A24-G26 and C65-G67 in PHGPx (Fig. 6A) and U2-U6, U10-A12, and U47-U50 in GPx (Fig. 6B). It is noteworthy that the window of interference for PHGPx was found to be much more compact than that found for GPx. One interpretation of this result is that the unique structure of the PHGPx SECIS, which contains an additional loop in helix 1, may enable SBP2 to bind in a fashion that requires fewer backbone phosphate groups. In ad-

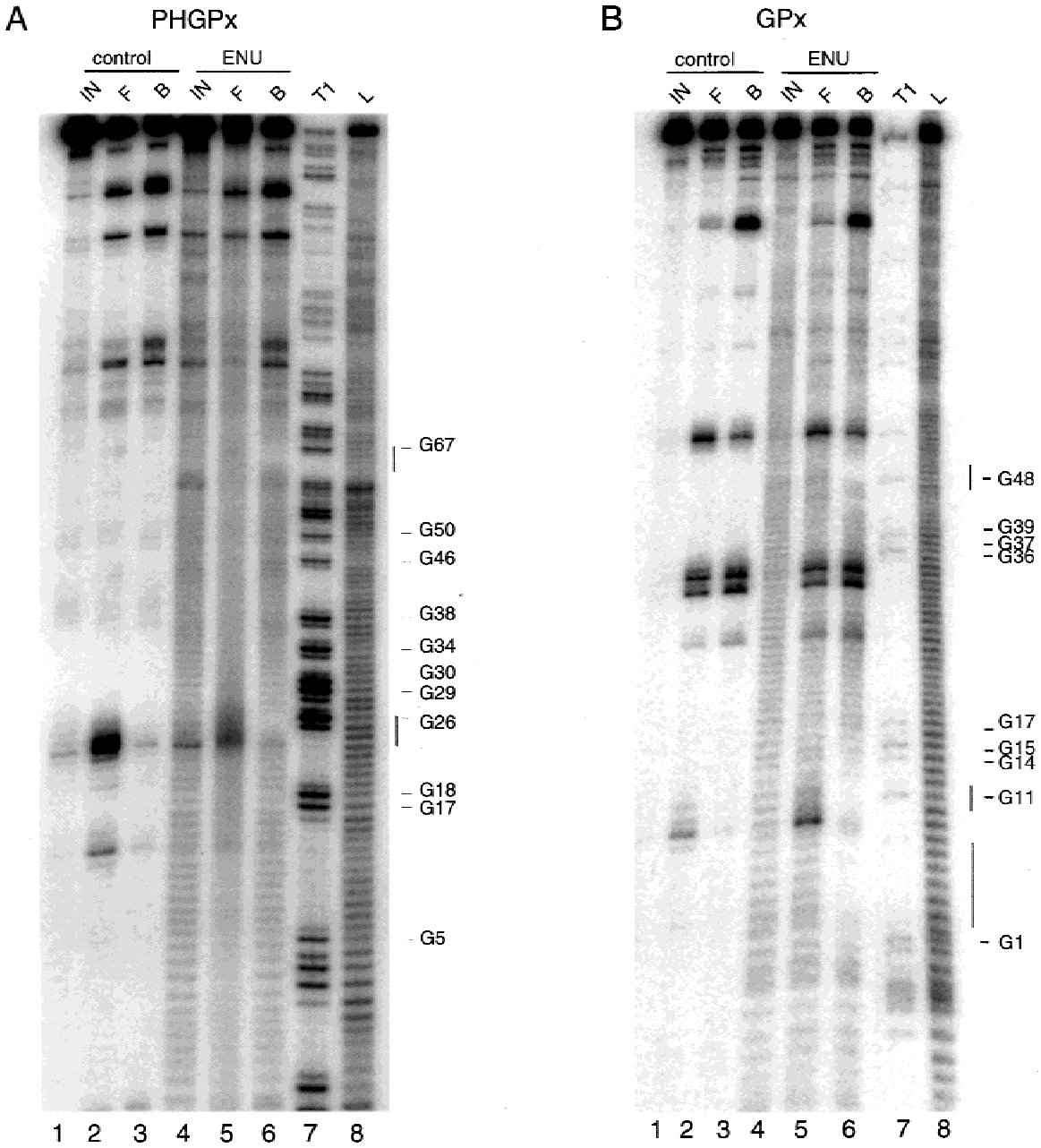

FIGURE 6. Ethylation interference analysis of SECIS RNA complex formation with SBP2. **A:** 5′-end-labeled untreated PHGPx SECIS RNA (control: lanes 1, 2, and 3) or RNA pretreated with ethylnitrosourea (ENU, lanes 4, 5, and 6) was used for complex formation with SBP2 and the bound and free RNAs were separated on native gels (see Materials and Methods). Lanes 1 and 4: input RNAs (IN); lanes 2 and 5 (F): free RNAs; lanes 3 and 6 (B): bound RNAs; lane 7: RNase T1 ladder (T1); Lane 8: alkaline ladder (L). The guanine positions correspond to the numbering in Figure 3; the positions in the SECIS RNA that interfere with binding to SBP2 are indicated on the right by bars. **B:** Determination of the GPx SECIS phosphates that interfere with the binding of SBP2, as described in **A**.

dition, the interference pattern for GPx is unique in that it contains phosphates in the 3′ strand of internal loop 1 that are protected from ethylation.

In the majority of the SBP2-SECIS RNA complexes that were analyzed, good correlation could be obtained between footprint experiments and the phosphate interference assay, enabling us to propose that the 5′ strands of helix 1 and part of internal loop 1, as well as all or part of the non-Watson–Crick base pairs, are involved in the interaction with SBP2. Due to minor differences found in the footprinting and interference patterns of individual SECIS elements, our data suggest that SBP2 may vary in its exact position around the SECIS core.

DISCUSSION

The eukaryotic selenocysteine incorporation machinery requires several gene products, including SBP2, the protein that interacts with the SECIS element, a hairpin in the 3′ UTR of selenoprotein mRNAs (Copeland & Driscoll, 1999; Copeland et al., 2000). In the course of characterizing this protein, two point mutations in the SECIS RNA core were previously described to abolish SBP2 binding. However, the mode of interaction between SBP2 and the SECIS RNA was not further investigated. In the work reported here, we have established that the recombinant rat SBP2 can bind to a variety of mammalian SECIS RNAs. Detailed biochemical probing of the interaction between SBP2 and SECIS RNAs has allowed us to define the binding site of SBP2. The analysis was further pursued making use of mutant forms of SECIS RNAs. Our findings correlate remarkably well with published structure/function studies dealing with the SECIS RNA and the SBP2-SECIS RNA interaction in vivo.

The mode of interaction between SBP2 and six different mammalian SECIS RNAs was examined by a combination of enzymatic and hydroxyl radical footprinting, phosphate-ethylation binding interference, and mobility shift analysis. Despite minor variations in the extent of the RNA regions protected and in the number and locations of the phosphates interfering with SBP2 binding in each individual RNA, the analyses provided an ensemble of data that are in congruence with each other. Thus, in the majority of the SECIS RNAs examined, riboses located on the 5′ strand of helix 1, as well as in the core of helix 2, were protected from hydroxyl radical modification by SBP2. Further, phosphates along the 5′ strand of helix 1 and along both strands of the bottom of helix 2, when modified, interfered with SBP2 binding. In a few SECIS RNAs, this was also the case for scattered phosphates in the 5′ strand of internal loop 1. This observation, combined with the deleterious effect of closing that loop, provides evidence that internal loop 1 is an important structural element for the interaction. From our data, we propose a model in which SBP2 envelopes the central part of the SECIS RNA, comprising the 5′ strands of helix 1 and internal loop 1, and the non-Watson–Crick base pair quartet (Fig. 7A). No other SECIS RNA region is required for SBP2 to bind. This finding is further strengthened by earlier experiments that allowed us to conclude that alteration of the apical sequences in the PHGPx SECIS was not detrimental to SBP2 binding (Lesoon et al., 1997; Copeland & Driscoll, 1999). Also, shortening of helix 2 by the removal of two G-C base pairs in the GPx SECIS did not affect SBP2 binding (data not shown). Taken together, our data show that there exists one single anchoring site for SBP2 on the SECIS RNA. Ethylation of a number of phosphates in helices 1 and 2, and internal loop 1 abrogated binding, suggesting that SBP2 may directly contact the RNA backbone at these positions. Alternatively, the inhibition of SBP2 binding could occur because of an indirect effect of the modification of some of the phosphates on the RNA structure itself. Nevertheless, our study highlights the prime importance of phosphates for SBP2 binding.

With regard to the RNA features recognized by SBP2, appealing are the dramatic lethal effects of substituting either the invariant U25 to C in PHGPx SECIS, or in the GPx SECIS the conserved G.A/A.G tandem to **A.G**/**G.A** or **A**.A/G.A, in contrast to the benignity of the G.A/A.**A** substitution. These findings correlate perfectly with previous data reporting that those same mutations impaired selenoprotein translation in vivo (Lesoon et al., 1997; Walczak et al., 1998), suggesting that this inhibition is very likely due to the inability of SBP2 to bind to the SECIS RNA. In structure-based sequence alignments, the G.A/A.G tandem in the non-Watson–Crick base pair quartet is strictly conserved throughout evolution (Walczak et al., 1996; Martin et al., 1998; Fagegaltier et al., 2000c). Therefore, both our experimental data and sequence comparisons support the notion that the G.A/A.G tandem represents a pivotal recognition element for SBP2. Although helix 1 and internal loop 1 were shown to be protected and/or to contain important phosphates, neither of these regions exhibit significant nucleotide sequence conservation in different SECIS RNAs. Interestingly, the three-dimensional structure model that was established for the SECIS RNA based on structure probing and computer modeling contains a sharp kink at internal loop 1 that serves as a hinge between helices 1 and 2 (Walczak et al., 1996). Figure 7B illustrates the proposed binding site of SBP2 on the three-dimensional model. This model shows that the non-Watson–Crick base pairs are accessible for interaction with SBP2 at the foot of helix 2, thereby explaining the necessity of internal loop 1, despite the lack of sequence conservation therein. In this loop, the A residue (numbered A9 in GPx SECIS) is invariant or replaced by G in only a few SECIS elements (Grundner-Culemann et al., 1999; Fagegaltier et al., 2000c). We have found in this work that the nature of the base at this position is not dramatically important to SBP2 binding, even though the protein protects the ribose and requires the phosphate 3′ to A9. Although surprising at first sight, this finding is in line with previous mutagenesis data showing that the A9G, C, or U changes did not alter significantly the ability of the GPx SECIS to mediate selenoprotein synthesis in vivo (Fagegaltier et al., 2000c).

Our binding analysis has also revealed that SBP2 does not discriminate between form 1 and form 2 SECIS elements. Previous analyses of SECIS element structures has shown that they fall into two classes: form 1 with an open apical loop, and form 2 with a closed apical loop (Grundner-Culemann et al., 1999; Fagegaltier et al., 2000c). Consistent with the data pre-

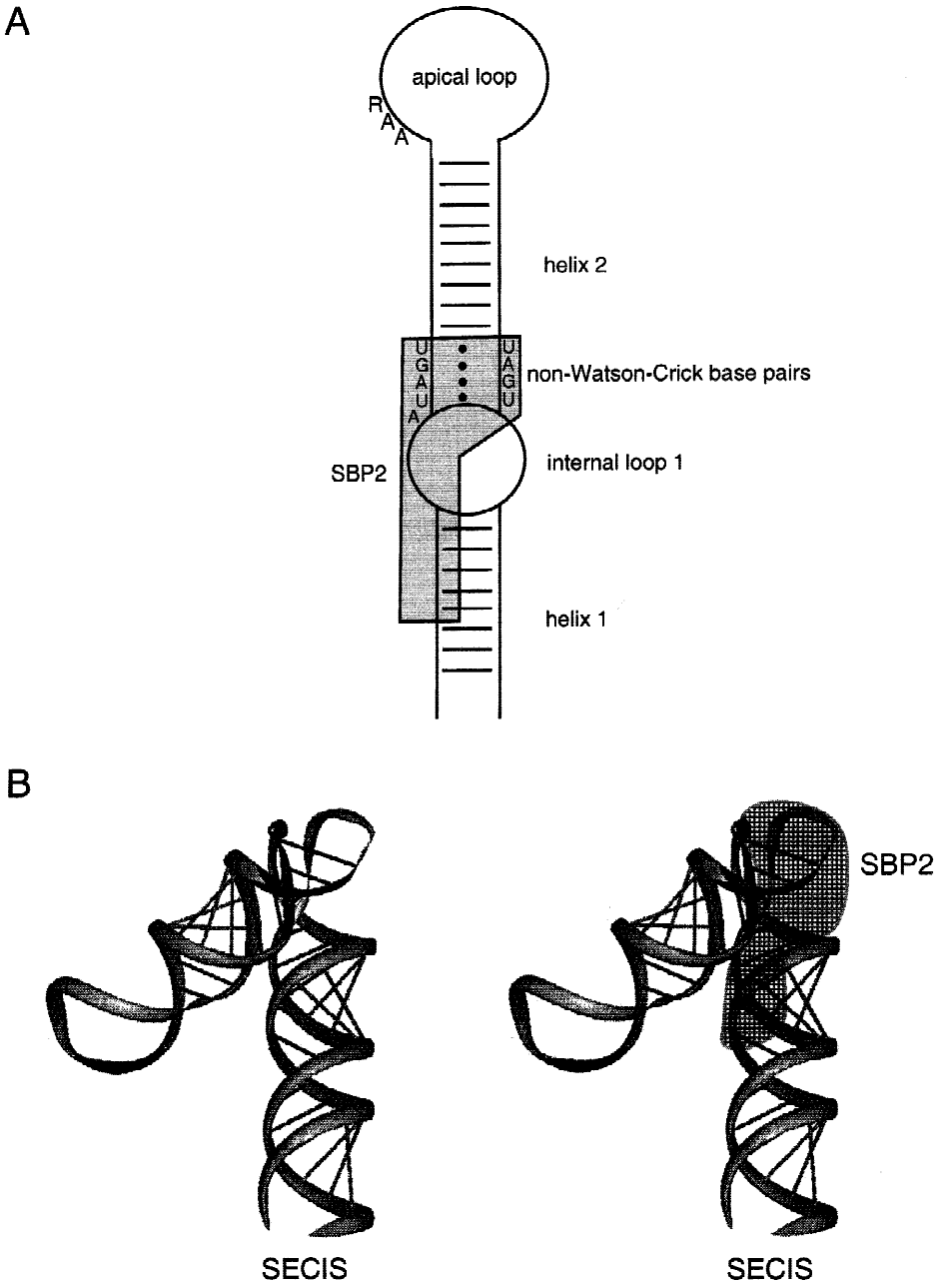

FIGURE 7. A model for the binding of SBP2 on the SECIS RNA. **A:** The SBP2-SECIS interaction is represented on the secondary structure of the rat 5′DI SECIS. The shaded box represents the regions with which SBP2 is likely to be in contact based on the results presented. **B:** The kink at the internal loop on the three-dimensional model of the rat 5′DI SECIS (shown in the left panel, after Walczak et al., 1996) exposes the non-Watson–Crick base pairs for interaction with SBP2 (schematized in the right panel), as discussed in the text.

sented here showing that SBP2 does not interact with the apex of the SECIS, the ability of SBP2 to bind the SECIS is not affected by the structure of the apical loop in either form 1 or form 2.

The apparent K_d values that we obtained for SBP2 ranged from approximately 100 to 200 nM. It is important to note that they represent data obtained in vitro, and thus may not reflect the absolute K_d values that would be observed in vivo. However, a comparison of the relative K_d values for SBP2 binding to various SECIS elements suggests that, although there are some differences, the range of affinities spanned only approximately twofold. This result is somewhat surprising because it has been proposed that SBP2 may be responsible for the hierarchy of selenoprotein expression observed in specific tissues and under conditions of limiting selenium (Low et al., 2000). The hierarchy of activity described in Low et al. (2000)

indicates that SBP2 is most effective with the first SECIS of SelP and least effective with the 5′ DI SECIS. Our results showed that SBP2 binds the 5′ DI SECIS and the PHGPx sequence with nearly equal affinity and the SelP SECIS with lower affinity. Although it is possible that SBP2 contributes to this phenomenon in vivo, it is clear from our results that the basis of its participation in the hierarchy is unlikely to involve its differential ability to bind SECIS elements without the participation of other yet unknown factors. Alternatively, the hierarchy might also be related to SBP2 in its potentially variable position centered around the SECIS core as shown by slight differences in the protection and interference patterns.

In conclusion, the results described above provide new insight into the mechanism of selenocysteine insertion by virtue of its detailed description of the SBP2/SECIS interaction. Of course, we find ourselves in the familiar position of being left with still more questions than answers. In addition to identifying nucleotides and structural features in the SECIS that are required for SBP2 binding, our data unambiguously demonstrate that SBP2 does not interact with the conserved AAR motif in the apical region, thus raising a poignant question regarding the function of this motif. Our current studies have thus far failed to identify a protein that specifically binds to this sequence (P.R. Copeland & D.M. Driscoll, unpubl. data), leaving us with the possibility that the apex of the SECIS RNA is interacting directly with the ribosome or perhaps the Sec-tRNA^{Sec} in performing its essential function in selenocysteine insertion.

MATERIALS AND METHODS

Constructs and in vitro transcription

The DNA constructs containing the rat PHGPx, wild-type or mutant rat GPx, rat 5′ DI, human SelN, and mouse Sel15 RNAs were constructed as described (Walczak et al., 1996, 1998; Fagegaltier et al., 2000c) The rat SelP construct was made by PCR-amplifying a 74-nt region corresponding to the first SECIS element using the following primers: TAATAC GACTCACTATAGGGTAGTTACATTGATGAGAACAG, which contains the T7 promoter at the 5′ end, and GCATGGATC CTAATTACGAGCTATCCAACAG, which contains a *Bam*HI site immediately 3′ to the end of the SECIS. Full-length rat SelP cDNA (kindly provided by K. Hill & R. Burk, Vanderbilt University) was used as the PCR template and the product was TA cloned into pUniV5-His-TOPO (Invitrogen). Prior to T7 transcription, plasmid DNAs were linearized with *Eco*RI (GPx, 5′ DI, SelN, and Sel15), *Hin*dIII (PHGPx), or *Bam*HI (SelP). Transcription by T7 RNA polymerase was conducted either as in Fagegaltier et al. (2000c) or in a modified Ribomax T7 (Promega) reaction. To produce 5′ ApG-ending RNAs for easier 5′-end labeling, 4 mM ApG was added and the GTP concentration was reduced to 1 mM, creating fragments of the following size: PHGPx: 203 nt; GPx: 121 nt; 5′ DI: 134 nt; SelN: 59 nt; Sel15: 67 nt; SelP: 74 nt. The 5′ ApG RNAs were 5′-end labeled with [γ ^{32}P]ATP, and purified on 15% denaturing polyacrylamide gels.

SBP2 purification

Purification of the recombinant C-terminal SBP2 protein was performed as described (Copeland et al., 2000), except that the elution buffer was exchanged to 20 mM Tris-acetate, pH 7.5, 50 mM potassium acetate, or phosphate buffered saline (PBS) and 2 mM DTT, using a 10 $\times$ 100 mm Fast Desalting column (AP biotech).

RNA protection

For the hydroxyl radical cleavages, 100,000 cpm of the 5′-end-labeled SECIS RNAs were used per reaction, and half that amount was used for the enzymatic cleavage reactions. In both hydroxyl radical-induced and enzymatic cleavage experiments, complex formation between the SECIS RNAs and recombinant C-terminal SBP2 was carried out in 20 μL of buffer A (2 mM DTT, 2.5 μg tRNA and 1$\times$ PBS). SBP2 was added to a final concentration ranging from 133 nM to 425 nM, or omitted. Reactions were incubated at 37 °C for 25 min. Fe(II)EDTA reactions were performed as described by Hüttenhofer and Noller (1992) with some modifications. After complex formation, the following was added to the reactions for a final volume of 25 μL: 4 mM EDTA, 10 mM DTT, 2 mM $(NH_4)_2Fe(S0_4)_2$, and 0.1% H_2O_2. Reactions were incubated for 4 min at room temperature.

RNase T1 and T2 cleavages were performed by adding 0.1 U of RNase T1 (Invitrogen) and 0.5 U of RNase T2 (Sigma) to the 20-μL preincubated reactions for 5 or 10 min at room temperature. All reactions were stopped by the addition of 80 μL of water and phenol-chloroform extraction. The ethanol precipitated RNAs were resuspended in water and RNA-loading dye. Samples were run on 8% sequencing gels. For RNase T1 ladders, 0.005 U of RNase T1 were added to 5′-end-labeled RNAs in 7 μL of 1$\times$ citrate buffer (25 mM sodium citrate, pH 5.5, 1 mM EDTA, 0.025% bromophenol blue, and 0.025% xylene cyanol), and the reaction was incubated at 55 °C for 10 min. Alkaline ladders were obtained by incubating the RNAs (containing 1 μg carrier tRNA) in 36 μL of 50 mM sodium carbonate, pH 8.9, for 5 min at 90 °C. The hydrolyzed RNAs were precipitated with 600 μL of 2% $LiClO_4$ in acetone. All RNA protection experiments yielded reproducible results in at least three independent experiments.

Ethylation interference

Ethylnitrosourea was used under conditions described by Romby et al. (1985), with a few modifications. We added 1 $\times$ 10^6 cpm of 5′-end-labeled SECIS RNA to 25 μL of ethylation buffer (100 mM cacodylate, pH 8.0, 1 mM EDTA, and 20% ethylnitrosourea-saturated ethanol solution) and incubated the sample for 1 min at 90 °C. The control reaction contained ethanol added to 20%. To stop the reactions, 75 μL of water were added and RNA was ethanol precipitated. Washed and dried pellets were raised in 10 μL of water, of which 3 μL was removed for use as the input fraction. The remaining 7 μL was added to a 20-μL binding reaction mix containing 1$\times$ PBS, 10 mM DTT, 50 μg soybean trypsin inhibitor (Sigma),

0.25 μg tRNA (Roche), and 0.25 μM SBP2. Binding reactions were incubated at 37 °C for 25 min, loading dye was added, and entire reactions were loaded on 4% nondenaturing gels. Bands corresponding to bound and unbound RNAs were cut from the gels and eluted overnight in elution buffer (500 mM ammonium acetate, pH 6.0, containing $\frac{1}{6}$ vol phenol). Following elution, the RNAs were phenol/chloroform extracted and ethanol precipitated. For hydrolysis of the RNA backbone, RNA pellets were dissolved in 10 μL of 0.1 M Tris-HCl, pH 9.0, and incubated for 10 min at 50 °C. The reaction was stopped with 90 μL of water and ethanol precipitated. Pellets were counted and equal counts were loaded on 8% sequencing gels. All ENU experiments yielded reproducible results in at least three independent experiments.

Mobility shift assay and K_d determination

The mobility shift assay was performed as described previously (Copeland et al., 2001), with [α-^{32}P]-labeled SECIS RNAs obtained by in vitro transcription with T7 RNA polymerase, according to Hubert et al. (1996). For the analysis of SECIS mutants, 150,000 cpm of RNA were used per binding assay. The intensity of the retarded complexes was quantitated by PhosphorImager analysis.

The apparent K_d for SBP2 binding (the concentration of SBP2 at half maximal RNA binding) was determined using the method described by Carey (1991). The amount of purified recombinant Strep-tagged SBP2 (Copeland et al., 2000) was varied from 7 to 140 nM for PHGPx and 5′ DI SECIS, 17.5 to 350 nM for SelN and Sel15 SECIS, and 35 to 700 nM for the GPx SECIS while keeping the amount of labeled RNA limiting at 250 pM. The unbound fraction of RNA was quantitated by PhosphorImager analysis and the amount of RNA remaining was plotted against SBP2 concentration. The linear portions of each curve were subjected to regression analysis, and the mean concentration plus/minus standard error for three experiments are reported.

ACKNOWLEDGMENTS

We are indebted to P. Romby for invaluable advice and technical comments regarding Fe/EDTA and ENU protocols. We are grateful to R. Burk and K. Hill for their generous gift of the full-length rat SelP construct. D. Fagegaltier and A. Lescure are thanked for fruitful discussions, and C. Loegler for excellent technical assistance. This work was supported by grants from the Ligue Régionale contre le Cancer, the Association pour la Recherche contre le Cancer (ARC) and the Centre Volvic pour la Recherche sur les Oligo-Eléments (to A.K.); by Public Health Service Grant HL 29582 (to D.M.D.) and by a Scientist Development Grant from the American Heart Association (to P.R.C.).

Received June 1, 2001; returned for revision June 25, 2001; revised manuscript received July 9, 2001

REFERENCES

Atkins JF, Gesteland RF. 2000. The twenty-first amino acid. *Nature 407*:463–465.

Berry MJ, Banu L, Chen YY, Mandel SJ, Kieffer JD, Harney JW, Larsen PR. 1991. Recognition of UGA as a selenocysteine codon in type I deiodinase requires sequences in the 3′ untranslated region. *Nature 353*:273–276.

Carey J. 1991. Gel retardation. *Methods Enzymol 208*:103–117.

Copeland PR, Driscoll DM. 1999. Purification, redox sensitivity, and RNA binding properties of SECIS-binding protein 2, a protein involved in selenoprotein biosynthesis. *J Biol Chem 274*:25447–25454.

Copeland PR, Fletcher JE, Carlson BA, Hatfield DL, Driscoll DM. 2000. A novel RNA binding protein, SBP2, is required for the translation of mammalian selenoprotein mRNAs. *EMBO J 19*:306–314.

Copeland PR, Stepanik VA, Driscoll DM. 2001. Insight into mammalian selenocysteine insertion: Domain structure and ribosome binding properties of Sec insertion sequence binding protein 2. *Mol Cell Biol 21*:1491–1498.

Fagegaltier D, Hubert N, Carbon P, Krol A. 2000a. The selenocysteine insertion sequence binding protein SBP is different from the Y-box protein dbpB. *Biochimie 82*:117–122.

Fagegaltier D, Hubert N, Yamada K, Mizutani T, Carbon P, Krol A. 2000b. Characterization of mSelB, a novel mammalian elongation factor for selenoprotein translation. *EMBO J 19*:4796–4805.

Fagegaltier D, Lescure A, Walczak R, Carbon P, Krol A. 2000c. Structural analysis of new local features in SECIS RNA hairpins. *Nucleic Acids Res 28*:2679–2689.

Fletcher JE, Copeland PR, Driscoll DM. 2000. Polysome distribution of phospholipid hydroperoxide glutathione peroxidase mRNA: Evidence for a block in elongation at the UGA/selenocysteine codon. *RNA 6*:1573–1584.

Fujiwara T, Busch K, Gross HJ, Mizutani T. 1999. A SECIS binding protein (SBP) is distinct from selenocysteyl-tRNA protecting factor (SePF). *Biochimie 81*:213–218.

Grundner-Culemann E, Martin GW III, Harney JW, Berry MJ. 1999. Two distinct SECIS structures capable of directing selenocysteine incorporation in eukaryotes. *RNA 5*:625–635.

Hubert N, Walczak R, Carbon P, Krol A. 1996. A protein binds the selenocysteine insertion element in the 3′-UTR of mammalian selenoprotein mRNAs. *Nucleic Acids Res 24*:464–469.

Hüttenhofer A, Noller HF. 1992. Hydroxyl radical cleavage of tRNA in the ribosomal P site. *Proc Natl Acad Sci USA 89*:7851–7855.

Lesoon A, Mehta A, Singh R, Chisolm GM, Driscoll DM. 1997. An RNA-binding protein recognizes a mammalian selenocysteine insertion sequence element required for cotranslational incorporation of selenocysteine. *Mol Cell Biol 17*:1977–1985.

Low SC, Grundner-Culemann E, Harney JW, Berry MJ. 2000. SECIS-SBP2 interactions dictate selenocysteine incorporation efficiency and selenoprotein hierarchy. *EMBO J 19*:6882–6890.

Martin GW, Harney JW, Berry MJ. 1998. Functionality of mutations at conserved nucleotides in eukaryotic SECIS elements is determined by the identity of a single nonconserved nucleotide. *RNA 4*:65–73.

Romby P, Moras D, Bergdoll M, Dumas P, Vlassov VV, Westhof E, Ebel JP, Giege R. 1985. Yeast tRNA^{Asp} tertiary structure in solution and areas of interaction of the tRNA with aspartyl-tRNA synthetase. A comparative study of the yeast phenylalanine system by phosphate alkylation experiments with ethylnitrosourea. *J Mol Biol 184*:455–471.

Shen Q, McQuilkin PA, Newburger PE. 1995. RNA-binding proteins that specifically recognize the selenocysteine insertion sequence of human cellular glutathione peroxidase mRNA. *J Biol Chem 270*:30448–30452.

Shen Q, Wu R, Leonard JL, Newburger PE. 1998. Identification and molecular cloning of a human selenocysteine insertion sequence-binding protein. A bifunctional role for DNA-binding protein B. *J Biol Chem 273*:5443–5446.

Tujebajeva RM, Copeland PR, Xu X-M, Carlson BA, Harney JW, Driscoll DM, Hatfield DL, Berry MJ. 2000. Decoding apparatus for eukaryotic selenocysteine insertion. *EMBO Rep 1*:158–163.

Walczak R, Carbon P, Krol A. 1998. An essential non-Watson–Crick base pair motif in 3′ UTR to mediate selenoprotein translation. *RNA 4*:74–84.

Walczak R, Westhof E, Carbon P, Krol A. 1996. A novel RNA structural motif in the selenocysteine insertion element of eukaryotic selenoprotein mRNAs. *RNA 2*:367–379.